Crystal Structure of the Aspartic Acid-199 → Asparagine Mutant of Chloramphenicol Acetyltransferase to 2.35-Å Resolution: Structural Consequences of Disruption of a Buried Salt Bridge[†,‡]

Michael R. Gibbs,[§] Peter C. E. Moody,[∥] and Andrew G. W. Leslie*[,§]

The Blackett Laboratory, Imperial College of Science, Technology, and Medicine, Prince Consort Road, London SW7 2BZ, U.K.

Received April 6, 1990; Revised Manuscript Received August 22, 1990

ABSTRACT: The crystal structure of the Asp-199 → Asn mutant of chloramphenicol acetyltransferase (CAT) has been determined to 2.35-Å resolution. In wild-type CAT Asp-199 is involved in a fully buried intrasubunit salt bridge with Arg-18, an interaction that is adjacent to the active site. Replacement of aspartate with asparagine by site-directed mutagenesis disrupts this salt bridge and causes extensive conformational changes within the active site. The imidazole group of the catalytically essential His-195 is reorientated, with the loss of interactions thought to stabilize the preferred tautomer of this residue. Arg-18 and Asn-199 form three new intersubunit interactions as a result of large side-chain torsion angle changes which cause the movement of two polypeptide loops, some residues of which are up to 20 Å away from the site of the mutation. The new interactions of Arg-18 and Asn-199 compensate for the loss of the buried salt bridge and afford near-wild-type thermostability to Asn-199 CAT, albeit with a greatly reduced activity.

Bacterial resistance to chloramphenicol (Cm)[1] is most commonly accounted for by the presence of the enzyme chloramphenicol acetyltransferase (CAT; EC 2.3.1.28), which catalyzes the acetylation of the antibiotic at the primary (C-3) hydroxyl (Shaw, 1983; Shaw & Leslie, 1989). The overall reaction (eq 1) is reversible although the formation of acetylated chloramphenicol and coenzyme A (CoA) is highly favored energetically.

$$\text{Cm} + \text{acetyl-CoA} \leftrightarrow \text{3-}O\text{-acetylchloramphenicol} + \text{CoA} \quad (1)$$

Genes encoding CAT are present in many bacterial genera and are frequently plasmid-borne (Shaw, 1983). There is a high degree of homology among the published amino acid sequences, with 27 residues absolutely conserved (Alton & Vapnek 1979; Shaw et al., 1979, 1985; Horinouchi & Weisblum, 1982; Harwood et al., 1983; Charles et al., 1985; Murray et al., 1988, 1989). Three plasmid-specific natural variants of CAT (I–III) have been identified in Gram-negative organisms (Foster & Shaw, 1973; Gaffney et al., 1978). The type III CAT variant (CAT_{III}) has been cloned into a high-level expression vector in *Escherichia coli* (30–50% of the soluble protein) (Murray et al., 1988) and has been characterized in detail. Kinetic studies support the formation of a ternary complex (CAT–Cm–AcCoA) in which both substrates bind independently (Kleanthous & Shaw, 1984). The active site directed inhibitor of CAT 3-(bromoacetyl)chloramphenicol was used to identify a conserved histidine (His-195)[2] which is essential for catalysis and is believed to act as a general base in the deprotonation of the primary hydroxyl of Cm (Kleanthous et al., 1985). His-195 is alkylated only at the NE2 atom of its imidazole ring, suggesting that the latter has a preferred tautomeric form (Kleanthous et al., 1985).

Crystallographic and hydrodynamic results showed CAT_{III} to be a trimer of three identical subunits with total M_r 75 000 (Leslie et al., 1986; Harding et al., 1987). Crystal structures of CAT_{III} complexed with chloramphenicol and coenzyme A have recently been determined at 1.75- and 2.4-Å resolution, respectively, revealing that the active sites are located at the subunit interfaces (Leslie et al., 1988). The two substrates approach the active site from opposite "sides" of the molecule, so that the combined substrate binding pockets form a remarkable channel that extends from one side of the trimer to the other. The conformation of His-195 within the active site is unusual as energetically unfavorable side-chain torsion angles are stabilized by an uncommon side chain to main chain hydrogen bond within this residue, and also by ring stacking with Tyr-25. In this conformation the preferred tautomer of the imidazole group favors its role as a general base.

Site-directed mutagenesis studies of CAT_{III} have focused upon identifying the roles of particular conserved residues in catalysis (Lewendon et al., 1988, 1990) and substrate binding (Shaw et al., 1988). The role of a conserved acidic residue, Asp-199, was investigated by replacing it with asparagine and alanine. Kinetic studies on these mutants suggested that Asp-199 has a structural rather than a direct catalytic role (Lewendon et al., 1988). This result is consistent with the crystal structure of the wild-type enzyme, which shows that Asp-199 forms an ion pair with the conserved residue Arg-18,

[†] A.G.W.L. and P.C.E.M. were supported by the Medical Research Council, U.K. M.R.G. received a Science and Engineering Research Council studentship.

[‡] Atomic coordinates for the Asn-199 mutant of chloramphenicol acetyltransferase have been deposited with the Brookhaven Protein Data Bank.

* Address correspondence to this author.

[§] Present address: MRC Laboratory of Molecular Biology, Cambridge CB2 2QH, U.K.

[∥] Present address: Department of Chemistry, University of York, Heslington, York YO1 5DD, U.K.

[1] Abbreviations: AcCoA, acetyl coenzyme A; Cm, chloramphenicol; CAT, chloramphenicol acetyltransferase; EDTA, ethylenediaminetetraacetic acid; MES, 2-(*N*-morpholino)ethanesulfonic acid; MPD, 2-methyl-2,4-pentanediol; rms, root mean square.

[2] Alignment of the amino acid sequences of type I, III, and C CAT variants has resulted in a general numbering system which is used here. The numbering here is related to the type III linear sequence by adding 5 to residues 1–74 and 6 to residues 75–213, such that His-195 and Asp-199 are residues 189 and 193, respectively, in the primary sequence of type III CAT (Murray et al., 1988).

0006-2960/90/0429-11261$02.50/0

an interaction that is entirely buried within the trimer (Leslie et al., 1988). Notably, this ion-pair interaction is adjacent to the imidazole ring of His-195. The guanidinium group of Arg-18 is also within hydrogen-bonding distance of the main-chain carbonyl oxygen atoms of residues 195 and 196. We report here the crystal structure of the Asn-199 CAT mutant to 2.35-Å resolution, in which the ion pair has been disrupted by substituting asparagine for aspartate. The structure reveals conformational changes of residues within the active site and at distances of up to 20 Å from the site of the mutation.

Materials and Methods

Single crystals were grown by microdialysis using small Lucite "buttons". Each button contained 30 μL of protein (5 mg/mL) in 10 mM MES, pH 6.3, and was dialyzed against 4 mL of 4% 2-methyl-2,4-pentanediol (MPD), 10 mM MES, pH 6.3, 1 mM Cm, 0.5 mM hexaamminecobalt(III) chloride, and 5 mM β-mercaptoethanol at 4 °C (Leslie et al., 1986). Crystals attained a maximum size of 300 × 300 × 300 μm^3 in 21 days and were harvested into the dialysate at 8% MPD. The mutant crystals were isomorphous with wild-type crystals (space group *R*32) with similar unit cell dimensions. Cell parameters of the equivalent hexagonal cell are a = 107.6 Å, c = 123.6 Å for wild type and a = 107.7 Å, c = 124.3 Å for Asn-199 CAT.

Crystallographic data were collected to 2.35-Å resolution at 4 °C on an Arndt–Wonacott oscillation camera on the Wiggler line at the Synchrotron Radiation Source at Daresbury, U.K., using radiation of wavelength 0.88 Å. The complete dataset (40°) was collected on two crystals and processed by using the MOSFLM program suite. Seven of the twenty-three film packs collected were rejected from the final dataset due to poor scaling with the remaining data, primarily as a result of crystal radiation damage. The resulting dataset comprised 75% of the unique data to 2.35 Å, which, with an average multiplicity of 2.3, gave a crystallographic merging R factor[3] of 7.8%.

The refined structure of the CAT–Cm binary complex was used as a starting model in refinement, with Asp-199 replaced by asparagine with identical torsion angles. An initial difference electron density map with coefficients $(|F_o| - |F_c|)$, α_c indicated substantial shifts for residues in two loops. The first of these two loops, involving residues 97–103, was deleted from the model and rebuilt at a later stage of refinement by using the "bones" option for main-chain tracing and the fragment fitting option (Jones & Thirup, 1986) of the interactive graphics program FRODO (Jones, 1978). The apparent movement of the second loop, comprising residues 13–18, was somewhat smaller and was considered to be within the radius of convergence of the refinement. The model was refined by using a version of the restrained parameter least-squares structure factor refinement program PROLSQ (Hendrickson & Konnert, 1980), in which the structure factor terms and their derivatives are calculated according to an algorithm based on fast Fourier transforms (Agarwal, 1978; Isaacs, 1982). Fourier maps with coefficients $(3|F_o| - 2|F_c|)$, α_c and $(|F_o| - |F_c|)$, α_c were used to rebuild several side chains which adopt quite different conformations in the mutant structure. Ten rounds of refinement, together with manual rebuilding, lowered the crystallographic R factor[4] from 25.7% to 15.2% and resulted in a model with good stereochemistry (Table I).

Table I: Stereochemistry of the Type III Asn-199 CAT Mutant Structure from *E. coli*

stereochemical refinement parameter	rms deviation from ideal values	refinement restraint weighting values
bond distance (Å)	0.02	0.02
angle distance (Å)	0.04	0.03
planar 1–4 distances (Å)	0.06	0.05
planes (Å)	0.02	0.02
chiral volumes (Å^3)	0.18	0.15
van der Waals contacts		
single torsion (Å)	0.16	0.20
multiple torsion (Å)	0.18	0.20

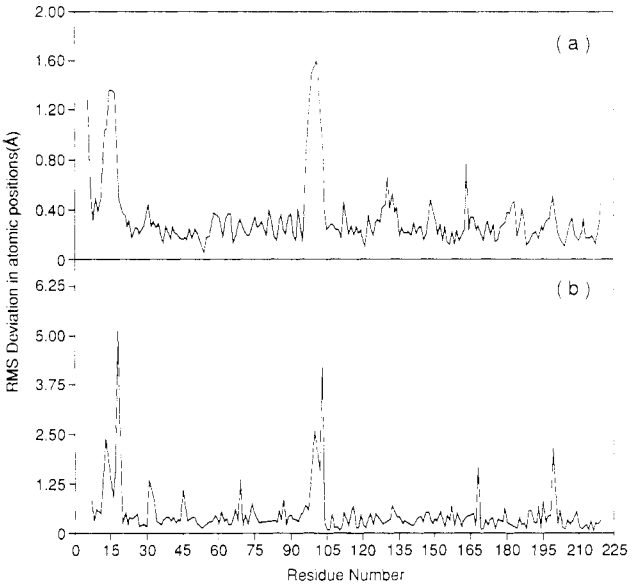

FIGURE 1: rms deviation of (a) main-chain and (b) side-chain coordinates between wild-type and Asn-199 CAT.

Results

A comparison of the refined mutant and wild-type structures shows that the aspartate to asparagine substitution causes conformational changes both locally in the active site and up to 20 Å away from the site of the point mutation.

The rms deviation in coordinates for main- and side-chain atoms between the wild-type and Asn-199 CAT proteins was 0.4 and 0.8 Å, respectively (Figure 1). The largest main-chain movements involve two polypeptide loops (residues 13–18 and 97–103). In the native structure these loops have mean main-chain temperature factors of 25 Å^2 and 18 Å^2, respectively, which, when compared to the value of 14 Å^2 for all residues in CAT, suggests that only the 13–18 loop is inherently flexible. These loops lie at the subunit interface, with residues 13–18 of one subunit packing against residues 97–103 of an adjacent subunit of the trimer. The first of these loops

[3] The merging R factor, R_{merge}, is defined as

$$R_{merge} = \frac{\sum\sum|I(h)i - \langle I(h)\rangle|}{\sum\sum I(h)i}$$

where $I(h)i$ is the scaled intensity for reflection h from the ith observation, $\langle I(h)\rangle$ is the weighted mean of all observations of reflection h, and the summation includes all observations.

[4] Progress of a structure refinement is monitored by a reliability index, R, defined as

$$R = \frac{\sum|F_{obs} - F_{calc}|}{\sum F_{obs}}$$

where F_{obs} and F_{calc} are the observed and calculated structure factor amplitudes, respectively.

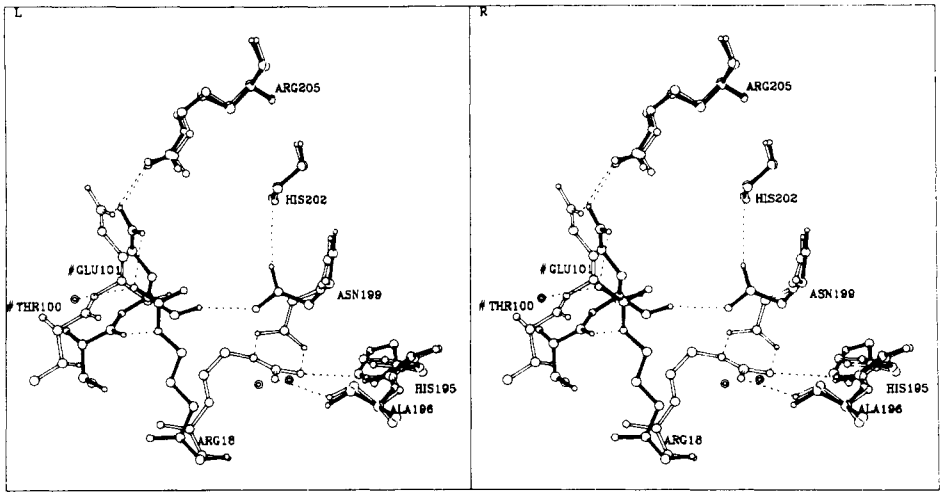

FIGURE 2: Stereoview showing the interactions of Arg-18 and Asp/Asn-199 side chains in wild-type (open bonds) and Asn-199 CAT (solid bonds). Double circles indicate water molecules in Asn-199 CAT, and dashed lines represent hydrogen bonds. Residue names preceded by # belong to an adjacent subunit of the trimer. Carbon, nitrogen, and oxygen atoms are represented by circles of decreasing size.

includes the conserved Arg-18 that forms the salt-bridge interaction with Asp-199 in wild-type CAT. The rms deviation for main-chain atoms is greater than 1 Å for both loops while that for the remaining residues in CAT is only 0.3 Å. The most prominent side-chain shifts are also found in these two loop regions. Important conformational changes also occur in the active site.

There was no evidence in the final electron density map for bound chloramphenicol, even though it was present at 1 mM concentration in the crystallization medium. It is likely that chemical modification of a reactive active site thiol, Cys-31, sterically precludes chloramphenicol from binding. A positive feature (0.27 e/Å^3) at a distance of 3.4 Å from the Cys-31 SG in the final electron density map can be interpreted as a β-mercaptoethanol molecule, a feature seen much more clearly in the Glu-199 CAT mutant (M. R. Gibbs and A. G. W. Leslie, unpublished experiments). Thus, Cys-31 appears to be at least partially modified by β-mercaptoethanol, in a similar manner to other thiol-specific reagents (Zaidenzaig & Shaw, 1978). It should be noted that similar modification of a thiol side chain has been reported for a T4 lysozyme mutant, although the β-mercaptoethanol molecule was not modeled into the electron density (Matsumura et al., 1989). The chloramphenicol binding site in Asn-199 CAT is occupied by five water molecules (441, 497, 498, 499, 503) which form a hydrogen-bonding network between themselves. Only water 498 forms a hydrogen bond to a protein atom (water 498···OH, Tyr-25 is 2.6 Å). While water 441 is common to both the apo-CAT and Asn-199 CAT structures, waters 498, 499, and 503 are unique to this mutant structure. These unique waters coincide with the β-mercaptoethanol molecule modeled into the apo-CAT structure (P. C. E. Moody and A. G. W. Leslie, unpublished experiments).

Conformational Changes. The aspartate to asparagine mutation replaces a side-chain carboxylate oxygen atom with an amino group, which can no longer accept the hydrogen bond from the NE of Arg-18 and therefore leads to the disruption of the Arg-18···Asp-199 salt bridge. In the structure of the mutant both these side chains adopt radically different conformations to those in the wild-type structure. The Asn-199 side-chain torsion angle χ_1 changes by 123°, and χ_3 of Arg-18 changes 121°, placing the guanidinium group at the subunit interface. These conformational changes lead to several new intra- and intersubunit interactions (Figure 2). In Asn-199 CAT one amino group of the Arg-18 side chain forms an intersubunit hydrogen bond with one of the carboxylate oxygens of Glu-101 (NH1, Arg-18···OE1, Glu-101 distance is 2.8 Å) and to a solvent molecule (water 484), while the NE of the guanidinium group hydrogen bonds across the subunit interface to the main-chain oxygen of Thr-100 (NE, Arg-18···O, Thr-100 distance is 2.9 Å) (Figure 2). Notably, the Arg-18 side chain is no longer within hydrogen-bonding distance of the main-chain carbonyl oxygen atoms of residues 195 and 196, as it is in the wild-type structures. Two new water molecules (waters 489 and 490) in the active site (exclusive to the Asn-199 CAT structure) occupy approximately the positions of the amino groups of the Arg-18 side chain in wild-type CAT. These waters form hydrogen bonds with the main-chain oxygen atoms of residues 195 and 196 (Figure 2). Additionally, one intersubunit hydrogen bond between the OE1 atom of Glu-101 and the NH1 of Arg-205 is lost but is replaced as the second carboxylate oxygen of Glu-101 becomes the hydrogen bond acceptor (OE2, Glu-101···NH1, Arg-205 is 2.7 Å) (Figure 2).

The orientation of the Asn-199 side chain allows it to make a number of new interactions (Figure 2). The first of these is a hydrogen bond between its side-chain oxygen and the main-chain nitrogen of His-202, a hydrogen-bonding geometry that is commonly observed in protein structures (Baker & Hubbard, 1984). The second interaction is a hydrogen bond between the amide nitrogen and the main-chain oxygen of Glu-101 of the 97–103 loop of the adjacent subunit. This interaction (O, Glu-101···ND2, Asn-199 is 2.7 Å) results in a 1-Å movement of the main-chain atoms of this loop (Figure 3). The shift of this loop results in two further changes. First, the side-chain torsion angle χ_1 of Phe-103 changes by 143° to avoid a steric clash with the side chain of Tyr-25 in the active site (Figure 4). Second, the residues in loop 13–18, which packs against the 97–103 loop of an adjacent subunit of the trimer, move to avoid the steric clash with the latter (Figure 3). In Asn-199 CAT both loops move to a similar extent and maintain their wild-type conformation, with the internal hydrogen bonds retained. These loop shifts represent the remote conformational changes in Asn-199 CAT, the greatest Cα–Cα distance being 20.0 Å (Asn-199···Lys-14).

Other active site residues have also moved, the most surprising of these being that of the His-195 side chain (Figure 4). In the structures of the apoenzyme as well as both binary complexes of the wild-type protein, the His-195 imidazole group ring-stacks with Tyr-25. In Asn-199 CAT His-195

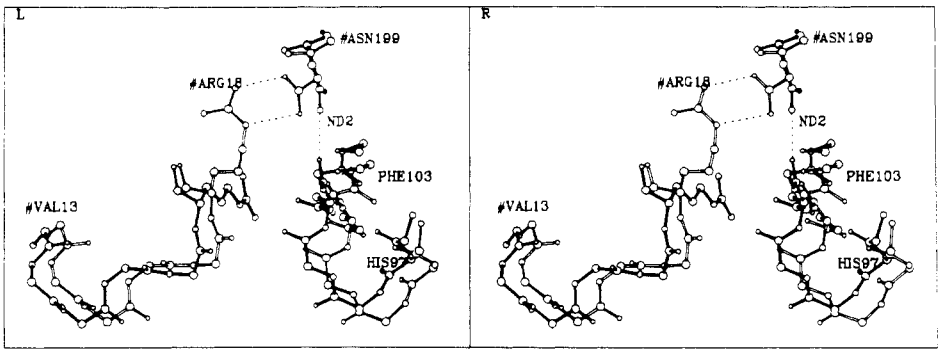

FIGURE 3: Stereoview showing the changes in loops 13–18 and 97–103 between the wild-type CAT (open bonds) and Asn-199 CAT structures (solid bonds). Residue names preceded by # belong to an adjacent subunit, and dashed lines represent hydrogen bonds.

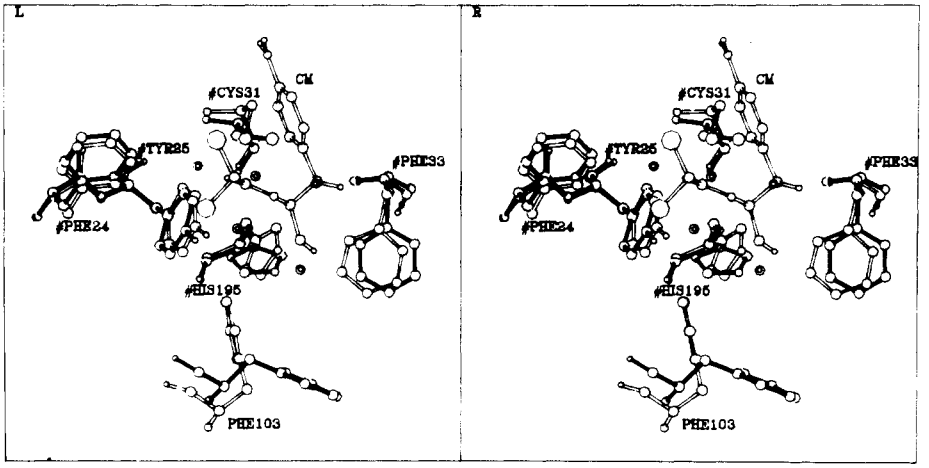

FIGURE 4: Stereoview showing the active site of wild-type (open bonds) and Asn-199 CAT (solid bonds) superimposed, with chloramphenicol (Cm) replaced by five new water molecules (double circles). Residue names preceded by # belong to an adjacent subunit.

adopts energetically more favorable side-chain torsion angles ($\chi_1 = -158°$, $\chi_2 = -98°$) than in wild-type CAT, as torsion angle χ_2 changes 48° such that the imidazole group forms an amino–aromatic interaction with Tyr-25, an interaction often seen in proteins (Burley & Petsko, 1986). This alters the geometry of the unusual hydrogen bond within His-195 that provides tautomeric stabilization of this side chain (the ND1···O distance drops by 0.2 Å to 2.7 Å, and the ND1-H···O angle changes −29° to 109°). The side chain of Tyr-25 undergoes only a small shift, while the Phe-33 side chain moves to avoid a steric clash with His-195 (Figure 4).

Discussion

The steady-state kinetic parameters (Table II) and thermostability (as measured by sensitivity to thermal inactivation) of three salt-bridge mutants of CAT (Asn-199 CAT, Ala-199 CAT, and Val-18 CAT) have been determined (Lewendon et al., 1988). Asn-199 CAT has a greatly reduced activity (k_{cat} is 0.28 s^{-1} compared to 599 s^{-1} for wild type) but shows very similar thermal stability to the wild-type enzyme, which is active and stable to prolonged incubation at 70 °C (Lewendon et al., 1988). Ala-199 and Val-18 CAT retain ~10% of wild-type activity but are rapidly and irreversibly inactivated at this temperature (Lewendon et al., 1988). Destabilization of Ala-199 and Val-18 CAT, reflected in their thermolabile nature, is probably due to the buried unpaired charges of Arg-18 and Asp-199, respectively, as suggested by Lewendon et al. (1988). They also propose that the thermostability of the Asn-199 CAT mutant could be attributed to new interactions that compensate for the loss of the salt bridge. The structure of Asn-199 CAT reported here supports the latter hypothesis and demonstrates that proteins may tolerate the loss of a buried salt bridge, provided that compensating, stabilizing interactions occur. In the case of Asn-199 CAT, these interactions include the formation of several new intersubunit hydrogen bonds, which result in the concerted movement of two polypeptide loops. The Glu-43 → Asp mutation in staphylococcal nuclease, which disrupts an active site salt bridge, is another example of a mutation that results in the movement of a polypeptide loop, although in this case the loop conformation is actually altered (Loll & Lattman, 1990).

Table II: Steady-State Kinetic Parameters for Wild-Type and Salt-Bridge Mutants of CAT[a]

CAT variant	k_{cat} (s^{-1})	K_M (μM)	
		Cm	AcCoA
wild type	599	11.6	93
Asn-199	0.28	46.5	314
Ala-199	45	14.5	83
Val-18	68	16.2	101

[a] Values taken from Lewendon et al. (1988).

In addition to the new intersubunit interactions, which involve the movement of two loops and the side chains of Arg-18 and Asn-199, there are significant differences in the side-chain conformations of two residues in the active site, Phe-103 and His-195. It is presumably the latter change that results in the dramatic loss in activity.

In the wild-type enzyme, Phe-103 forms part of the binding pocket that accommodates the β-mercaptoethylamine moiety of AcCoA (Leslie et al., 1988). In Asn-199 CAT this side chain completely blocks this binding pocket. The binding of AcCoA to Asn-199 CAT cannot, however, differ from that in native CAT, given the nature of the AcCoA-binding site

and the mere 3-fold increase in the K_M for AcCoA (from 93 μM to 314 μM). The Phe-103 side chain must, therefore, adopt a new conformation when AcCoA binds to Asn-199 CAT. This in turn will require some rearrangement of other residues in the active site.

The observed change in the conformation in the His-195 side chain is less dramatic, but potentially far more deleterious to catalysis. In wild-type CAT, the His-195 side chain adopts energetically unfavorable torsion angles ($\chi_1 = -145°$, $\chi_2 = -36°$), which allows the formation of a hydrogen bond between the imidazole ND1 and the main-chain carbonyl oxygen of His-195. A search of the Brookhaven Data Bank has revealed no other examples of this type of interaction. In Asn-199 CAT the His-195 side chain adopts more favorable torsion angles ($\chi_1 = -158°$, $\chi_2 = -98°$), but the reason for this change is not immediately apparent. Modeling studies show that the histidine could adopt the wild-type conformation without making unfavorable van der Waals contacts with neighboring residues. Cys-31, which is believed to be at least partially modified by β-mercaptoethanol (see Results), is in the neighborhood of His-195 and could influence the side-chain orientation. The same thiol modification, however, is observed in the native apo-CAT and CAT–CoA structures where the histidine orientation is unchanged, which indicates that the alternative conformation of His-195 seen in Asn-199 CAT cannot be due to this modified Cys-31. An alternative explanation is associated with the strength of the hydrogen bond between the imidazole ND1 and carbonyl oxygen of His-195, which is likely to be influenced by the interaction between this main-chain carbonyl oxygen and the amino group of Arg-18 (NH2, Arg-18···O, His-195 distance is 3.1 Å). The positive charge of the guanidinium group will increase the electronegativity of the carbonyl oxygen, which in turn will strengthen the interaction between the carbonyl oxygen and the imidazole ND1. In Asn-199 CAT the interaction between the carbonyl oxygen and Arg-18 no longer exists but is replaced by a hydrogen bond to a water molecule unique to Asn-199 CAT (O, His-195···O, water 490 distance is 2.8 Å). This may then account for the observed change in orientation of the His-195 side chain; the reduced electronegativity of the carbonyl oxygen will weaken the ND1–carbonyl oxygen hydrogen bond so that it can no longer stabilize the unfavorable torsion angles that are required for this interaction. In the conformation observed in Asn-199 CAT, there is no apparent mechanism for stabilization of the preferred tautomeric form of the histidine, which offers an explanation of the reduced catalytic competence of this mutant.

ACKNOWLEDGMENTS

We thank Professor W. V. Shaw and Drs. A. Lewendon and I. A. Murray (Department of Biochemistry, University of Leicester, U.K.) for advice on preparation of the manuscript and the gift of the Asn-199 CAT protein, the preparation and characterization of which was supported by a research grant from the Protein Engineering Initiative of the Biotechnology Directorate of the Science and Engineering Research Council, U.K. We also thank the SERC Daresbury Laboratory, U.K., for access to the synchrotron.

Registry No. Asp, 56-84-8; Asn, 70-47-3.

REFERENCES

Agarwal, R. C. (1978) *Acta. Crystallogr., Sect. A 34*, 791.
Alton, N. K., & Vapnek, D. (1979) *Nature (London) 282*, 864.
Baker, E. N., & Hubbard, R. E. (1984) *Prog. Biophys. Mol. Biol. 44*, 97.
Burley, S. K., & Petsko, G. A. (1986) *FEBS Lett. 203*, 139.
Charles, I. G., Keyte, J. W., & Shaw, W. V. (1985) *J. Bacteriol. 164*, 123.
Foster, T. J., & Shaw, W. V. (1973) *Antimicrob. Agents Chemother. 3*, 99.
Gaffney, D. F., Foster, T. J., & Shaw, W. V. (1978) *J. Gen. Microbiol. 109*, 351.
Harding, S. E., Rowe, A. J., & Shaw, W. V. (1987) *Biochem. Soc. Trans. 15*, 513.
Harwood, C. R., Williams, D. M., & Lovett, P. S. (1983) *Gene 24*, 163.
Hendrickson, W. A., & Konnert, J. H. (1980) in *Computing in Crystallography* (Diamond, R., Ramaseshan, S., & Venkatesan, K., Eds.) p 13.01, National Academy of Sciences, India, Bangalore, India.
Horinouchi, S., & Weisblum, B. (1982) *J. Bacteriol. 150*, 815.
Isaacs, N. W. (1982) in *Computational Crystallography* (Sayre, D., Ed.) pp 398, Clarendon Press, Oxford.
Jones, A. T. (1978) *J. Appl. Crystallogr. 11*, 268.
Jones, A. T., & Thirup, S. (1986) *EMBO J. 5*, 819.
Kleanthous, C., & Shaw, W. V. (1984) *Biochem. J. 223*, 211.
Kleanthous, C., Cullis, P. M., & Shaw, W. V. (1985) *Biochemistry 24*, 5307.
Leslie, A. G. W., Liddell, J. M., & Shaw, W. V. (1986) *J. Mol. Biol. 188*, 283.
Leslie, A. G. W., Moody, P. C. E., & Shaw, W. V. (1988) *Proc. Natl. Acad. Sci. U.S.A. 85*, 4133.
Lewendon, A., Murray, I. A., Kleanthous, C., Cullis, P. M., & Shaw, W. V. (1988) *Biochemistry 27*, 7385.
Lewendon, A., Murray, I. A., Shaw, W. V., Gibbs, M. R., & Leslie, A. G. W. (1990) *Biochemistry 29*, 2075.
Loll, P. J., & Lattman, E. E. (1990) *Biochemistry 29*, 6866.
Matsumura, M., Wozniak, J. A., Dao-pin, S., & Matthews, B. W. (1989) *J. Biol. Chem. 264*, 16059.
Murray, I. A., Hawkins, A. R., Keyte, J. W., & Shaw, W. V. (1988) *Biochem. J. 252*, 173.
Murray, I. A., Gil, J. A., Hopward, D. A., & Shaw, W. V. (1989) *Gene 85*, 283.
Shaw, W. V. (1983) *CRC Crit. Rev. Biochem. 14*, 1.
Shaw, W. V., & Leslie, A. G. W. (1989) in *Handbook of Experimental Pharmacology* (Bryan, L. E., Ed.) p 313, Springer-Verlag.
Shaw, W. V., Packman, L. C., Burleigh, B. D., Dell, A., Morris, H. R., & Hartley, B. S. (1979) *Nature (London) 282*, 870.
Shaw, W. V., Brenner, D. G., Le Grice, S. F. J., Skinner, S. E. & Hawkins, A. R. (1985) *FEBS Lett. 179*, 101.
Shaw, W. V., Day, P., Lewendon, A., & Murray, I. A. (1988) *Biochem. Soc. Trans. 16*, 939.
Zaidenzaig, Y., & Shaw, W. V. (1978) *Eur. J. Biochem. 83*, 553.